Renormalized Coupled-Cluster Calculations of Reactive Potential Energy Surfaces: The BeFH System†

Michael J. McGuire,‡ Piotr Piecuch,*,‡,§,|| Karol Kowalski,‡ Stanisław A. Kucharski,‡,⊥ and Monika Musiał⊥

Department of Chemistry, Michigan State University, East Lansing, Michigan 48824, and Institute of Chemistry, University of Silesia, Szkolna 9, 40-006 Katowice, Poland

Received: March 12, 2004; In Final Form: May 28, 2004

The completely renormalized (CR) CCSD(T) method has been used to calculate the entire ground-state potential energy surface (PES) for the Be + HF reaction on a grid of nuclear geometries consisting of ∼3000 points. The cc-pVTZ and cc-pVQZ basis sets have been employed. In addition to the case of the Be atom approaching the HF molecule from the fluorine side and the case of the Be atom approaching HF from the hydrogen side, several values of the Be−F−H angle and the insertion of the Be atom between the H and F atoms of HF have been examined. The CR-CCSD(T) results have been compared with the results of CCSD(T) and multireference configuration interaction (MRCI) calculations. It has been demonstrated that the ground-state PES of the BeFH system obtained from the single-reference "black-box" CR-CCSD(T) calculations is in excellent agreement with the PES obtained from the expensive MRCI calculations, whereas the PES resulting from the standard CCSD(T) calculations is qualitatively incorrect and characterized by large errors relative to MRCI on the order of several electronvolts.

Introduction

The Be + HF reaction has been the subject of several theoretical studies, including calculations of the ground-state potential energy surfaces (PES) for the BeFH system with diatomics-in-molecules,[1] density functional theory,[2] and the configuration interaction (CI) approach,[2−4] as well as fitting the PES to different functional forms[3−7] and calculations of reaction dynamics.[3,6] Being the lightest member of an important family of exchange reactions involving alkaline earth metals and halides,[8−19] the Be + HF reaction serves as an excellent test case for new theoretical methods, particularly new electronic structure methods that are aimed at describing PESs involving breaking and making of chemical bonds.

A new class of "black-box" ab initio methods, based on the coupled-cluster (CC) wave function ansatz[20−24] and employing the method of moments of coupled-cluster equations (MMCC),[25−32] termed the renormalized CC approaches,[25−28,30−33] has recently been developed with the intention of removing the pervasive failing of the standard single-reference CC approximations, such as CCSD[34] and CCSD(T),[35] in the region of large internuclear separations. It has been demonstrated that the renormalized CC methods using the spin- and symmetry-adapted restricted Hartree−Fock (RHF) or restricted open-shell Hartree−Fock (ROHF) references, including, among others, the completely renormalized CCSD(T) (CR-CCSD(T)) approach,[25−28,30−33] are capable of describing unimolecular dissociations,[25−28,30−33,36,37] diradicals,[38] and highly excited vibrational states near the dissociation threshold.[28,30,32,36,37]

McGuire et al.[39] have shown that the CR-CCSD(T) approach may also be capable of removing the failing of the standard RHF-based single-reference CC methods in calculations of multidimensional PESs describing exchange chemical reactions of the A + BC → AB + C type. They used the CR-CCSD(T) method to calculate the PES for the collinear Be + HF → BeF + H reaction and compared the results with the exact PES obtained in the full CI calculations and the PES obtained in the CCSD(T) calculations[39] (see also refs 30−32). Because of the use of the full CI approach, the calculations reported in ref 39 were performed with a very small MIDI basis set,[40] and the PES scan was limited to the collinear arrangement of the Be, F, and H atoms, with Be approaching HF from the fluorine side. It has been demonstrated that the CR-CCSD(T) approach provides remarkable improvements in the poor description of the PES of the BeFH system by the CCSD(T) approach, but several questions remain open. First, the use of a small basis set may cause the small errors in the results of the CR-CCSD(T) calculations relative to full CI to be artificially low because of the unsatisfactory description of the relevant dynamic correlation effects by a small number of virtual orbitals in the basis set. Second, it is important to know if the small errors observed in the CR-CCSD(T) calculations for the collinear Be + HF → BeF + H reaction, reported in ref 39, remain equally small if we examine other reaction channels, including the insertion of Be into the H−F bond (see, for example, refs 2, 4, and 7), the case of the Be atom approaching HF from the hydrogen side, and other angles of approach of the HF molecule by Be.

The above questions are examined in this article. We extend the earlier and rather limited small basis set study[39] by considering the entire three-dimensional PES of the BeFH system, including the Be atom approaching the HF molecule from both the fluorine and hydrogen sides, several values of the Be−F−H angle, and the insertion of Be between the H and

† Part of the "Gert D. Billing Memorial Issue".

* To whom correspondence should be addressed. E-mail: piecuch@cem.msu.edu. Internet: www.cem.msu.edu/∼piecuch/group_web.

‡ Michigan State University.

§ Alfred P. Sloan Research Fellow.

|| Also at: Department of Physics and Astronomy, Michigan State University, East Lansing, MI 48824.

⊥ University of Silesia.

10.1021/jp048880h CCC: $27.50
Published on Web 07/07/2004

F atoms. The CR-CCSD(T) calculations are performed with the realistic cc-pVTZ and cc-pVQZ basis sets.[41] The CR-CCSD(T) results are compared with the standard CCSD and CCSD(T) results on one hand and the highly accurate results of the multireference CI (MRCI) calculations on the other hand. By comparing the CR-CCSD(T) results with the results of applying the sophisticated MRCI approach, which is often used to obtain highly accurate PESs for studies of small molecule reaction dynamics, we can learn if the single-reference CR-CCSD(T) approach, which preserves the ease-of-use and the relatively low computer cost of the CCSD(T) approximation, can compete with the MRCI method in applications involving multidimensional PESs. By comparing the CR-CCSD(T) results with those obtained with the standard CCSD and CCSD(T) approaches, we can learn about the level of improvement of the poor CCSD and CCSD(T) results in the region of larger internuclear separations offered by the CR-CCSD(T) approach. Finally, by comparing the results obtained with the cc-pVTZ and cc-pVQZ basis sets, and by comparing the results obtained in this work with the results obtained earlier[39] with the small MIDI basis set, we can examine the effect of the basis on the relative performance of the CCSD, CCSD(T), and CR-CCSD(T) methods in calculations of reactive PESs.

Theory and Computational Details

The Renormalized and Completely Renormalized CCSD(T) Approaches. The renormalized CC methods, including CR-CCSD(T), are derived by considering the noniterative corrections to standard CC energies that define the MMCC formalism.[25−32] These corrections are expressed in terms of the generalized moments of CC equations defining a given CC approximation, i.e., the CC equations projected on the excited configurations that are not included in the standard CC calculations. In the specific case of the CR-CCSD(T) approach, we consider the projections of the CCSD equations on triply excited configurations to construct the relevant MMCC energy correction to the CCSD energy.

The CR-CCSD(T) energy can be given the following compact forms:[25−28,30−33,37]

$$E^{\mathrm{CR-CCSD(T)}} = E^{\mathrm{CCSD}} + N^{\mathrm{CR(T)}}/D^{\mathrm{(T)}} \tag{1}$$

where E^{CCSD} is the CCSD energy,

$$N^{\mathrm{CR(T)}} = \langle\Phi|(T_3^{[2]} + Z_3)^{\dagger} M_3(2)|\Phi\rangle \tag{2}$$

and

$$D^{\mathrm{(T)}} = 1 + \langle\Phi|T_1^{\dagger}T_1|\Phi\rangle + \left\langle\Phi\middle| T_2^{\dagger}\left(T_2 + \frac{1}{2}T_1^{2}\right)\middle|\Phi\right\rangle + \left\langle\Phi\middle|(T_3^{[2]} + Z_3)^{\dagger}\left(T_1T_2 + \frac{1}{6}T_1^{3}\right)\middle|\Phi\right\rangle \tag{3}$$

with T_1 and T_2 representing the singly and doubly excited clusters obtained in the CCSD calculations employing $|\Phi\rangle$ as a reference configuration (throughout the present article, we assume that $|\Phi\rangle$ is a ground-state RHF determinant). The quantity $M_3(2)|\Phi\rangle$, entering eq 2, is defined as

$$M_3(2)|\Phi\rangle = \sum_{\substack{a<b<c\\ i<j<k}} \mathscr{M}_{abc}^{ijk}(2)|\Phi_{ijk}^{abc}\rangle \tag{4}$$

where

$$\mathscr{M}_{abc}^{ijk}(2) = \langle\Phi_{ijk}^{abc}|[H_{\mathrm{N}}\exp(T_1 + T_2)]_{\mathrm{C}}|\Phi\rangle \tag{5}$$

are the triply excited moments of the CCSD equations or the CCSD equations projected on the triply excited determinants $|\Phi_{ijk}^{abc}\rangle$ relative to reference $|\Phi\rangle$, $H_{\mathrm{N}} = H - \langle\Phi|H|\Phi\rangle$ is the electronic Hamiltonian in the normal product form, and C designates the connected part of a given operator expression (as usual, the letters i, j, k (a, b, c) label the spin−orbitals that are occupied (unoccupied) in the reference determinant $|\Phi\rangle$). The $T_3^2|\Phi\rangle = R_0^{(3)}(V_{\mathrm{N}}T_2)_{\mathrm{C}}|\Phi\rangle$ and $Z_3|\Phi\rangle = R_0^{(3)}V_{\mathrm{N}}T_1|\Phi\rangle$ terms, entering eqs 2 and 3, where $R_0^{(3)}$ is the three-body part of the many-body perturbation theory (MBPT) reduced resolvent and V_{N} is the two-body part of H_{N}, are the connected and disconnected wave function contributions due to triple excitations defining the standard CCSD(T) theory.[35]

The CR-CCSD(T) method reduces to the standard CCSD(T) approach if the denominator $D^{\mathrm{(T)}}$, eq 3, is replaced by 1 and if the numerator $N^{\mathrm{CR(T)}}$, eq 2, is replaced by the leading term

$$N^{\mathrm{(T)}} = \langle\Phi|(T_3^{[2]} + Z_3)^{\dagger}(V_{\mathrm{N}}T_2)_{\mathrm{C}}|\Phi\rangle \tag{6}$$

The approximation of $D^{\mathrm{(T)}}$ by 1 is justifiable, provided that the T_1 and T_2 cluster amplitudes are small, which is usually the case for the nondegenerate electronic states (e.g., molecules near their equilibrium geometries), for which the MBPT series rapidly converges. In fact, one can easily show[25,26,32] that $D^{\mathrm{(T)}}$ equals 1 plus terms that are at least of the second order in the perturbation V_{N} (see eq 3). The situation changes when the configurational quasi-degeneracy or nondynamic correlation effects become sizable and the MBPT series no longer converges, as is usually the case for stretched nuclear geometries. In this case, the T_1 and T_2 clusters become large and $D^{\mathrm{(T)}}$ becomes substantially larger than 1.[25,26] This increase in the values of $D^{\mathrm{(T)}}$ at larger internuclear distances is one of the main reasons for the excellent performance of the CR-CCSD(T) approach in the bond-breaking region, since large $D^{\mathrm{(T)}}$ denominators damp the excessively large negative values of the noniterative triples corrections $N^{\mathrm{(T)}}$, eq 6, resulting from the standard CCSD(T) calculations at stretched nuclear geometries, which cause the poor description of bond breaking by the CCSD(T) method (see, for example, refs 25 and 26 for further discussion). The presence of the $D^{\mathrm{(T)}}$ denominator in the CR-CCSD(T) energy formula, eq 1, causes the CR-CCSD(T) approach to not be strictly size extensive, but it has been demonstrated that the departure from strict size extensivity that these denominators produce does not exceed ~0.5% of the total correlation energy. This is a small price to pay considering the significant improvements that the renormalized CC methods offer in the bond-breaking region compared to the rigorously size-extensive and failing CCSD(T) approach (see refs 30 and 39 for further discussion). It is also worth mentioning that the use of the simplified numerator $N^{\mathrm{(T)}}$, eq 6, instead of the full numerator $N^{\mathrm{CR(T)}}$, eq 2, in eq 1 leads to the renormalized CCSD(T) method, abbreviated as R-CCSD(T).[25−28,30−33,37] Although in this article we focus on the performance of the more complete CR-CCSD(T) approach, the ground-state energies of the BeFH system obtained with the R-CCSD(T) method are provided too (see the Supporting Information). The R-CCSD(T) method offers considerable improvements in the CCSD(T) results for stretched nuclear geometries, but in general the R-CCSD(T) approach is not as robust as the CR-CCSD(T) method when larger internuclear separations are considered.[25−28,30,33,37]

The apparently simple relationships between the renormalized and completely renormalized CCSD(T) methods and their standard CCSD(T) counterpart immediately imply that the computer costs of the R-CCSD(T) and CR-CCSD(T) calcula-

tions are essentially identical to the costs of the standard CCSD(T) calculations. Thus, in analogy to the standard CCSD(T) method, the R-CCSD(T) and CR-CCSD(T) approaches are $n_o^3 n_u^4$ procedures in the noniterative steps involving triples and $n_o^2 n_u^4$ procedures in the iterative CCSD steps (n_o and n_u are the numbers of occupied and unoccupied orbitals, respectively, employed in the correlated calculations). The CR-CCSD(T) approach is twice as expensive as the standard CCSD(T) approach in the steps involving noniterative triples corrections, whereas the cost of the R-CCSD(T) calculation is the same as the cost of the CCSD(T) calculation.[37] The memory and disk storage requirements characterizing the R-CCSD(T) and CR-CCSD(T) methods are essentially identical to those characterizing the standard CCSD(T) approach. Apart from the relatively low computer cost of the R-CCSD(T) and CR-CCSD(T) approaches, the main practical advantage of these methods is the fact that they are as easy to use as the standard "black-box" approaches of the CCSD(T) type, while allowing us to considerably improve the description of the bond-breaking region without the need to define active orbitals or using other elements of multireference theory.

The Remaining Computational Details. All CC calculations for the BeFH system reported in this article, including the CCSD, CCSD(T), R-CCSD(T), and CR-CCSD(T) calculations, were performed using the suite of RHF-based CC programs described in ref 37. These programs are an integral part of the GAMESS package.[42] The MRCI calculations were carried out using the internally contracted MRCI(Q) approach including the quasi-degenerate Davidson corrections and employing the complete active space self-consistent field (CASSCF) reference, developed by Werner and Knowles[43,44] and implemented in the MOLPRO package.[45] The active space used in the MRCI(Q) calculations consisted of eight active orbitals with eight active electrons that correlate with the 2s and 2p shells of Be, the 2p shell of F, and the 1s orbital of the H atom. The core orbital correlating with the 1s shell of the fluorine atom was kept frozen in all of the above calculations.

The CCSD, CCSD(T), R-CCSD(T), CR-CCSD(T), and MRCI(Q) calculations for BeFH were performed using the cc-pVTZ and cc-pVQZ basis sets.[41] The cc-pVTZ basis set was used to calculate the entire three-dimensional PES of the BeFH system. Because of the large costs of the MRCI(Q) calculations and the large number of geometries included in our calculations, the cc-pVQZ basis set was only used to examine the collinear Be + HF → BeF + H reaction.

The three-dimensional PESs for the BeFH system were determined by performing the CCSD, CCSD(T), R-CCSD(T), CR-CCSD(T), and MRCI(Q) calculations on a grid of 2852 nuclear geometries defined as follows. For the six values of the Be−F−H angle θ ranging from 45° to 180° (θ = 45°, 70°, 80°, 90°, 135°, and 180°; θ = 180° represents a collinear arrangement of the Be, F, and H atoms, with F located between Be and H), we used the following values of the Be−F and H−F distances, R_{Be-F} and R_{H-F}, respectively: R_{Be-F} = 1.8, 1.9, 2.0, 2.2, 2.4, 2.5, 2.5719, 2.6, 2.7, 2.9, 3.1, 3.3, 3.5, 3.7, 3.9, 4.1, 4.5, 4.7, 5.0, 5.2, 5.5, 6.0, and 8.0 bohr, and R_{H-F} = 1.2, 1.4, 1.6, 1.7325, 1.8, 2.0, 2.25, 2.5, 2.75, 3.0, 3.5, 4.0, 5.0, 6.0, and 8.0 bohr. For the value of θ = 0° corresponding to the beryllium atom approaching the hydrogen atom of the HF molecule, the CCSD, CCSD(T), R-CCSD(T), CR-CCSD(T), and MRCI(Q) energies were calculated for the Be−H distances R_{Be-H} = 1.8, 1.9, 2.0, 2.2, 2.4, 2.5, 2.52, 2.6, 2.7, 2.9, 3.1, 3.3, 3.5, 3.7, 3.9, 4.1, 4.5, 4.7, 5.0, 5.2, 5.5, 6.0, and 8.0 bohr, and the H−F distances R_{H-F} = 1.2, 1.4, 1.6, 1.7325, 1.8, 2.0, 2.25, 2.5, 2.75, 3.0, 3.5, and 4.0 bohr. Finally, for the value of θ = 0° corresponding to the beryllium atom inserted between the hydrogen and fluorine atoms, the bond distances were chosen as R_{Be-F} = 1.8, 1.9, 2.0, 2.2, 2.4, 2.5, 2.5719, 2.6, 2.7, 2.9, 3.1, 3.3, 3.5, 3.7, 3.9, 4.1, 4.5, 4.7, 5.0, 5.2, 5.5, and 6.0 bohr, and R_{Be-H} = 1.8, 1.9, 2.0, 2.2, 2.4, 2.5, 2.52, 2.6, 2.7, 2.9, 3.1, 3.3, 3.5, 3.7, 3.9, 4.1, 4.5, 4.7, 5.0, 5.2, 5.5, 6.0, and 8.0 bohr. Notice the presence of the approximate equilibrium bond lengths of the BeF, HF, and BeH molecules (2.5719, 1.7325, and 2.52 bohr, respectively[46]) among the values of R_{Be-F}, R_{H-F}, and R_{Be-H} defining our basic grid. In the PES regions of special importance, for example, in the saddle point region, many additional points were considered.

All values of θ, R_{Be-F}, R_{Be-H}, and R_{H-F}, and the corresponding CCSD, CCSD(T), R-CCSD(T), CR-CCSD(T), and MRCI(Q) energies obtained with the cc-pVTZ and cc-pVQZ basis sets can be found in the Supporting Information.

Results and Discussion

We divide the discussion of the results into a few subsections corresponding to different types of arrangements of the Be, F, and H atoms (collinear, bent, etc., as defined by different values of the Be−F−H angle θ). We also have a separate subsection discussing the θ dependence of the saddle point energies and a subsection comparing the results obtained in this study using the cc-pVTZ and cc-pVQZ basis sets with the results obtained earlier[39] with the small, MIDI,[40] basis set. The main focus of our discussion is the performance of the CCSD and CCSD(T) vs MRCI(Q) and CR-CCSD(T) vs MRCI(Q) methods.

The PES for the Collinear Be + HF → BeF + H Reaction (θ = 180°) Obtained with the cc-pVTZ Basis Set. The ground-state PESs of the BeFH system, as described by the cc-pVTZ basis set, obtained in the CCSD(T), CR-CCSD(T), and MRCI(Q) calculations for θ = 180°, are shown in Figure 1. The maximum values of the absolute errors, relative to MRCI(Q), characterizing the CCSD, CCSD(T), and CR-CCSD(T) PESs of the BeFH system when the Be−F−H angle θ is fixed at 180°, resulting from the calculations with the cc-pVTZ basis set, can be found in Table 1.

As shown in Figure 1 and Table 1, the CCSD and CCSD(T) PESs differ greatly from the MRCI(Q) PES, while the CR-CCSD(T) PES is almost identical to the MRCI(Q) PES. The CCSD and CCSD(T) PESs show very large differences with the MRCI(Q) PES, especially in the region where both the Be−F and H−F bonds are stretched. For the value of θ = 180° discussed here, the differences between the CCSD(T) and MRCI(Q) energies are greater (in absolute value) than 1 eV in the entire $R_{Be-F} \geq 5.5$ bohr and $R_{H-F} \geq 6.0$ bohr region. They are greater than 0.5 eV in the entire $R_{Be-F} \geq 5.0$ bohr and $R_{H-F} \geq 5.0$ bohr region, and they exceed 0.2 eV for almost all nuclear geometries from the $R_{Be-F} < 2.5$ bohr and $R_{H-F} \geq 2.5$ bohr region, for the majority of geometries from the $R_{Be-F} \geq 3.5$ bohr and $R_{H-F} \geq 3.5$ bohr region, and for many geometries from the 2.5 bohr $\leq R_{Be-F} < 3.5$ bohr and $R_{H-F} \approx 3.0$ bohr region. The maximum difference between the CCSD(T) and MRCI(Q) energies of the collinear BeFH system, as described by the cc-pVTZ basis set, is 3.269 eV (cf. Table 1 and Figure 1d), which clearly shows how serious the breakdown of the RHF-based CCSD(T) approximation can be in studies of chemical reactions. Similar remarks apply to the CCSD calculations. For example, the differences between the CCSD and MRCI(Q) energies are greater than 0.5 eV in the entire $R_{Be-F} \geq 3.9$ bohr and $R_{H-F} \geq 4.0$ bohr region and for almost all geometries from the $R_{Be-F} < 3.9$ bohr and 2.5 bohr $\leq R_{H-F} <$

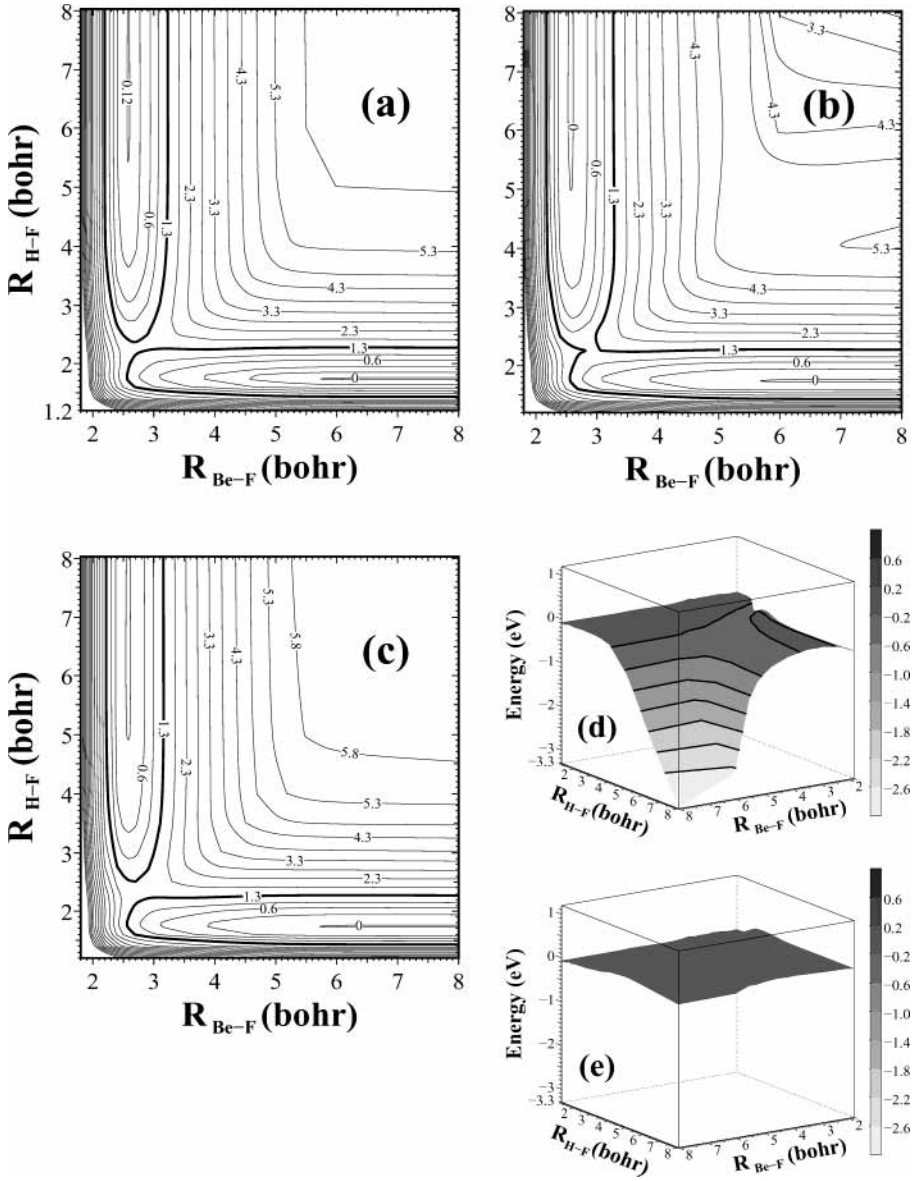

Figure 1. Contour plots for the ground-state PES of the BeFH system, as described by the cc-pVTZ basis set, at $\theta = 180°$, calculated with the MRCI(Q) (a), CCSD(T) (b), and CR-CCSD(T) (c) methods and the dependence of the differences between the CCSD(T) and MRCI(Q) (d) and CR-CCSD(T) and MRCI(Q) (e) energies for $\theta = 180°$ on the Be−F and H−F internuclear separations, R_{Be-F} and R_{H-F}, respectively. All energies are reported in electronvolts relative to the Be + HF reactants ($R_{Be-F} = 50.0$ bohr and $R_{H-F} = 1.7325$ bohr). The thick contour line at 1.3 eV, shown in (a−c), separates the region where the contour spacing is 0.3 eV from the region where the contour spacing is 0.5 eV. An extra contour line corresponding to 0.12 eV has been added to (a) to better describe the product channel. The error energy scales on the right side of (d) and (e) are in electronvolts.

TABLE 1: Maximum Absolute Errors (in Electronvolts), Relative to MRCI(Q) (the cc-pVTZ and cc-pVQZ basis sets) and Full CI (the MIDI basis set), in the CCSD, CCSD(T), and CR-CCSD(T) Energies for the Ground-State PES of the BeFH System at a Be−F−H Angle θ of 180°[a]

			maximum absolute error					
basis set	method	all geometries	$R_{Be-F} \le 3.1$	$3.1 < R_{Be-F} \le 5.0$	$5.0 < R_{Be-F}$	$R_{H-F} \le 3.0$	$3.0 < R_{H-F} \le 5.0$	$5.0 < R_{H-F}$
cc-pVTZ[b]	CCSD	1.137	0.641	0.767	1.137	0.641	0.844	1.137
	CCSD(T)	3.269	0.467	0.629	3.269	0.442	0.794	3.269
	CR-CCSD(T)	0.180	0.173	0.180	0.149	0.173	0.158	0.180
cc-pVQZ[b]	CCSD	1.250	0.689	0.838	1.250	0.689	0.907	1.250
	CCSD(T)	4.077	0.530	0.638	4.077	0.443	0.812	4.077
	CR-CCSD(T)	0.198	0.181	0.198	0.169	0.181	0.174	0.198
MIDI[c]	CCSD	0.443	0.277	0.443	0.356	0.199	0.358	0.443
	CCSD(T)	0.778	0.236	0.759	0.778	0.204	0.264	0.778
	CR-CCSD(T)	0.085	0.045	0.085	0.066	0.036	0.081	0.085

[a] The R_{Be-F} and R_{H-F} values are in bohr. [b] This work. [c] Taken from ref 39.

4.0 bohr region. As shown in Table 1, the maximum difference between the CCSD and MRCI(Q) results is 1.137 eV. Thus, the standard CCSD and CCSD(T) methods lead to huge errors relative to MRCI(Q) when the ground-state PES of BeFH is

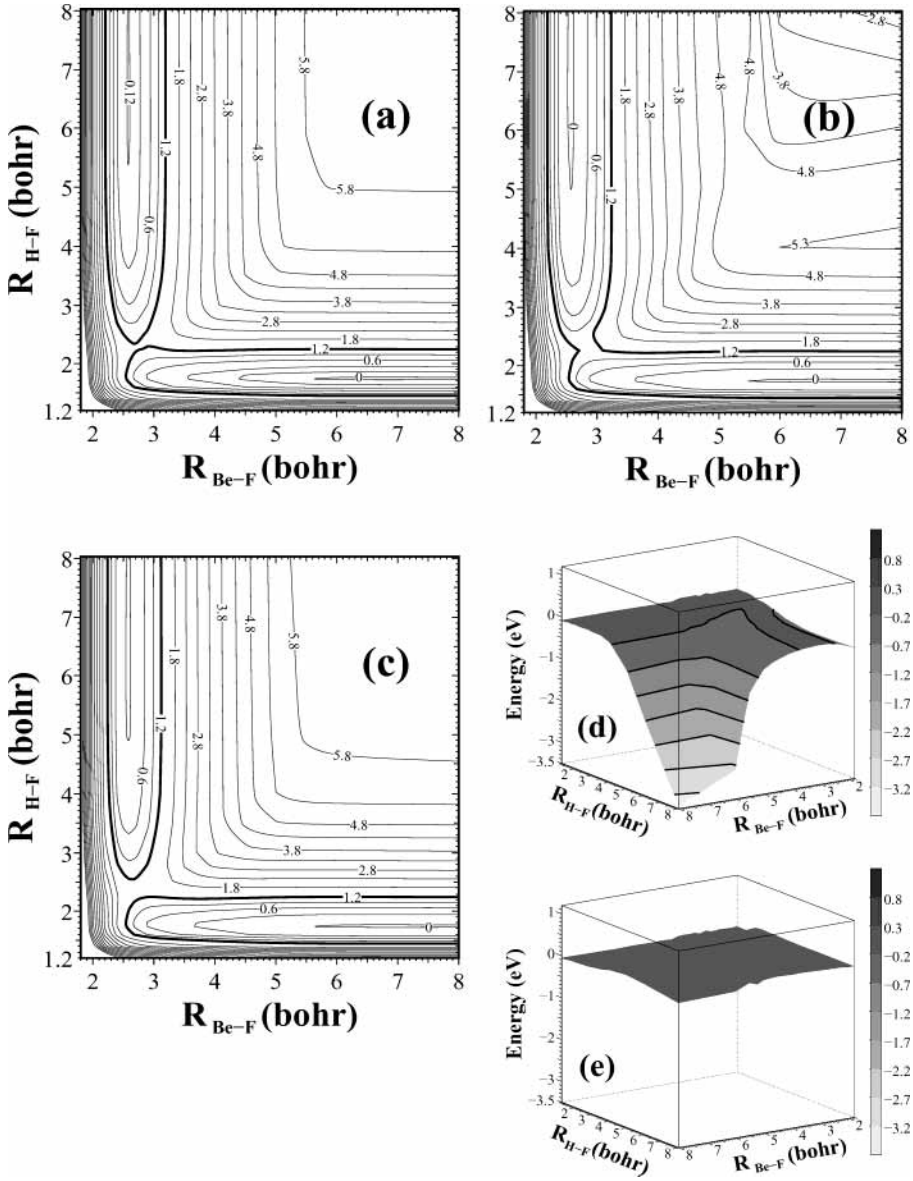

Figure 2. Contour plots for the ground-state PES of the BeFH system, as described by the cc-pVTZ basis set, at $\theta = 135°$ calculated with the MRCI(Q) (a), CCSD(T) (b), and CR-CCSD(T) (c) methods and the dependence of the differences between the CCSD(T) and MRCI(Q) (d) and CR-CCSD(T) and MRCI(Q) (e) energies for $\theta = 135°$ on the Be−F and H−F internuclear separations, R_{Be-F} and R_{H-F}, respectively. All energies are reported in electronvolts relative to the Be + HF reactants ($R_{Be-F} = 50.0$ bohr and $R_{H-F} = 1.7325$ bohr). The thick contour line at 1.2 eV, shown in (a−c), separates the region where the contour spacing is 0.3 eV from the region where the contour spacing is 0.5 eV. An extra contour line corresponding to 0.12 eV has been added to (a) to better describe the product channel. The error energy scales on the right side of (d) and (e) are in electronvolts.

examined. The only essential difference between the CCSD and CCSD(T) results is the fact that the PES obtained in the CCSD calculations is located above the MRCI(Q) PES, whereas the CCSD(T) PES is located below the MRCI(Q) PES.

The poor performance of the CCSD and CCSD(T) methods should be contrasted with the excellent performance of the CR-CCSD(T) approach for which the errors relative to MRCI(Q) are less than 0.2 eV when $\theta = 180°$ (see Figure 1e and Table 1). Typically, the differences between the CR-CCSD(T) and MRCI(Q) energies for the collinear ($\theta = 180°$) BeFH system, as described by the cc-pVTZ basis set, are on the order of 0.01−0.1 eV. In other words, the CR-CCSD(T) and MRCI(Q) PESs are virtually parallel and lie very close to each other (see Figure 1e; see also Figures 1a,c and Table 1). The CR-CCSD(T) PES is located slightly above the MRCI(Q) PES, so that the CR-CCSD(T) approach eliminates the nonvariational collapse of the standard CCSD(T) method at larger internuclear separations. The excellent performance of the CR-CCSD(T) approach and the parallelity of the CR-CCSD(T) and MRCI(Q) PESs are in sharp contrast with a highly nonuniform distribution of differences between the CCSD(T) and MRCI(Q) energies and large errors in the CCSD(T) results relative to MRCI(Q) shown in Figure 1d. The only region where the CCSD and CCSD(T) methods give relatively small errors is the region of smaller Be−F and H−F distances, but even there the overall performance of the CR-CCSD(T) approach is superior. For example, the CR-CCSD(T) method reduces the relatively large 0.4−0.6 eV maximum errors in the CCSD and CCSD(T) results in the $R_{Be-F} \leq 3.1$ bohr and $R_{H-F} \leq 3.0$ bohr region to less than 0.2 eV (often, 0.01−0.1 eV). It is quite remarkable to observe that the differences between the CR-CCSD(T) and MRCI(Q) energies remain consistently small for all values of R_{Be-F} and R_{H-F}.

A close inspection of the saddle point region of the CCSD(T) PES for $\theta = 180°$ shows that this part of the CCSD(T) PES is

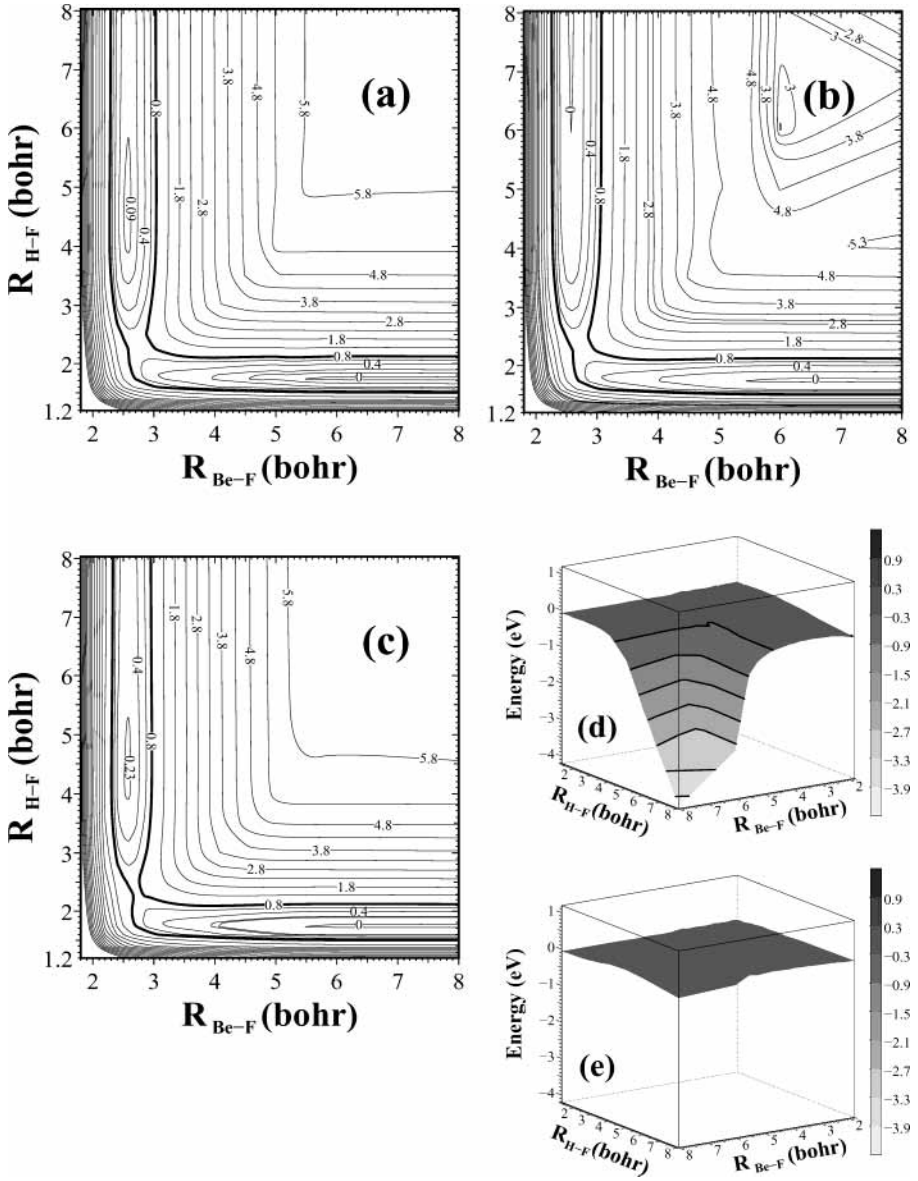

Figure 3. Contour plots for the ground-state PES of the BeFH system, as described by the cc-pVTZ basis set, at $\theta = 90°$, calculated with the MRCI(Q) (a), CCSD(T) (b), and CR-CCSD(T) (c) methods and the dependence of the differences between the CCSD(T) and MRCI(Q) (d) and CR-CCSD(T) and MRCI(Q) (e) energies for $\theta = 90°$ on the Be−F and H−F internuclear separations, R_{Be-F} and R_{H-F}, respectively. All energies are reported in electronvolts relative to the Be + HF reactants ($R_{Be-F} = 50.0$ bohr and $R_{H-F} = 1.7325$ bohr). The thick contour line at 0.8 eV, shown in (a−c), separates the region where the contour spacing is 0.2 eV from the region where the contour spacing is 0.5 eV. Extra contour lines corresponding to 0.09, 3, and 0.23 eV have been added to (a), (b), and (c), respectively, to better characterize important PES regions. The error energy scales on the right side of (d) and (e) are in electronvolts.

located below the corresponding part of the MRCI(Q) PES. This can be seen by comparing the thick contour lines corresponding to an energy of 1.3 eV in Figure 1a,b. The CCSD(T) PES allows for the formation of the BeF + H products at lower energies than the MRCI(Q) PES. This should be contrasted with the fact that the saddle point region on the CR-CCSD(T) PES is located slightly above the saddle point region on the MRCI(Q) PES. We will return to the discussion of the saddle point energies obtained in the CCSD(T), CR-CCSD(T), and MRCI(Q) calculations in the last subsection of this section.

In general, the CR-CCSD(T) approach eliminates the undesirable unphysical features on the PES produced by the CCSD(T) method at intermediate and large stretches of the H−F and Be−F bonds. For example, the CCSD(T) PES creates a false impression of the existence of a well-pronounced barrier leading to the formation of the Be + F + H atomic products, which is an artifact of the CCSD(T) calculations. The CR-CCSD(T) PES does not have this problem (cf. the $R_{H-F} > 4.0$ bohr and $R_{Be-F} > 5.0$ bohr region on the MRCI(Q), CCSD(T), and CR-CCSD(T) PESs shown in Figure 1a−c, respectively). Also, the shallow van der Waals well in the product (BeF + H) valley is located on the CCSD(T) PES below the Be + HF reactants, which is wrong (cf. the CCSD(T) PES in Figure 1b with the MRCI(Q) PES in Figure 1a). As shown in Figure 1c, the CR-CCSD(T) method eliminates this problem too. Clearly, the overall description of the product channel by the CCSD(T) method is not correct. For example, the endothermicity of the Be + HF → BeF + H reaction of −0.009 eV, obtained with the CCSD(T) method, has the wrong sign when compared to the MRCI(Q) endothermicity of 0.140 eV or the MRCI value reported by Aguado et al.[2] of 0.26 eV. The CR-CCSD(T) endothermicity value of 0.284 eV, although somewhat above the MRCI(Q) value, retains the correct sign and is in excellent agreement with the MRCI result reported in ref 2. The CR-

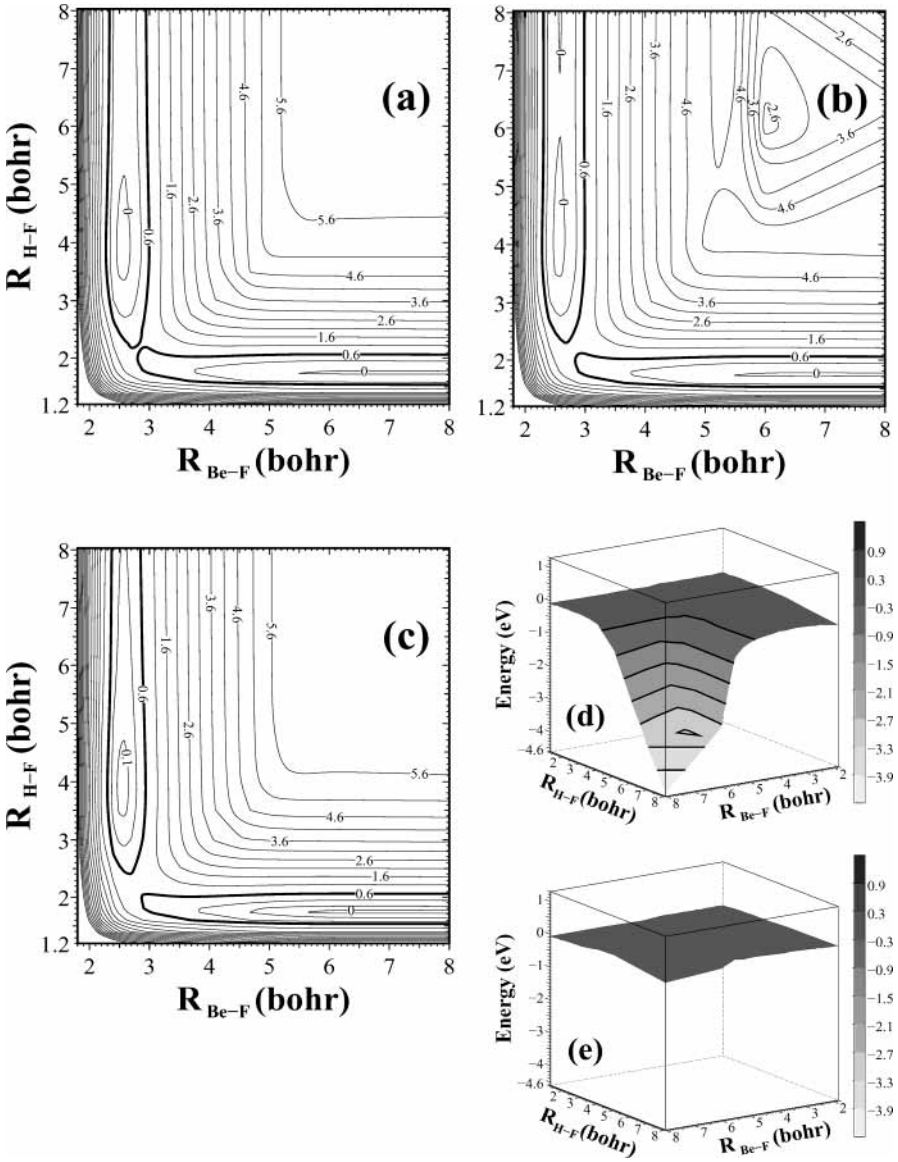

Figure 4. Contour plots for the ground-state PES of the BeFH system, as described by the cc-pVTZ basis set, at $\theta = 80°$, calculated with the MRCI(Q) (a), CCSD(T) (b), and CR-CCSD(T) (c) methods and the dependence of the differences between the CCSD(T) and MRCI(Q) (d) and CR-CCSD(T) and MRCI(Q) (e) energies for $\theta = 80°$ on the Be−F and H−F internuclear separations, R_{Be-F} and R_{H-F}, respectively. All energies are reported in electronvolts relative to the Be + HF reactants ($R_{Be-F} = 50.0$ bohr and $R_{H-F} = 1.7325$ bohr). The thick contour line at 0.6 eV, shown in (a−c), separates the region where the contour spacing is 0.3 eV from the region where the contour spacing is 0.5 eV. An extra contour line corresponding to 0.1 eV has been added to (c) to better describe the product channel. The error energy scales on the right side of (d) and (e) are in electronvolts.

CCSD(T) result for the endothermicity of the Be + HF → BeF + H reaction is also in very good agreement with the experimentally derived value of 0.193 eV, obtained using the experimental data for the binding energies of HF[47] and BeF.[48] The product (BeF + H) valley and the Be + F + H asymptotic region of the CR-CCSD(T) PES obtained with the cc-pVTZ basis set are shaped in almost exactly the same way as the product valley and the Be + F + H region of the MRCI(Q) PES. This can be best seen by comparing the thick contour lines corresponding to 1.3 eV and thin contour lines corresponding to 5.3 and 5.8 eV in Figure 1a,c. These contour lines have incorrect shapes when the CCSD(T) PES is examined (see Figure 1b). Unlike in the MRCI(Q) and CR-CCSD(T) cases, the contour line corresponding to 5.3 eV on the CCSD(T) PES is located only in the narrow region of large Be−F and intermediate H−F distances. The energy value of 5.8 eV above the reactants is never reached in the CCSD(T) calculations (the maximum CCSD(T) energy relative to the Be + HF reactants in Figure 1b is ca. 5.4 eV). This should be contrasted with the fact that the contour line at 5.8 eV is clearly seen on the MRCI(Q) and CR-CCSD(T) PESs shown in Figure 1a,c, respectively.

The Ground-State PES of the BeFH System for $\theta = 135°$, 90°, 80°, 70°, and 45° Obtained with the cc-pVTZ Basis Set. The results of the CCSD, CCSD(T), CR-CCSD(T), and MRCI(Q) calculations for the ground-state PES of the BeFH system in which the Be−F−H angle θ is fixed at 135°, 90°, 80°, 70°, and 45° are summarized in Figures 2−6 and Table 2. For each of these angles, the PESs calculated using the CCSD and CCSD(T) approaches show large deviations from the PES calculated with the MRCI(Q) method. As in the case of $\theta = 180°$, the largest errors are observed in the region of stretched Be−F and H−F bonds. In the case of the CCSD method, the maximum error, relative to MRCI(Q), for θ ranging between 45° and 180°, is 1.284 eV, although there seems to be little dependence of the differences between the CCSD and MRCI(Q)

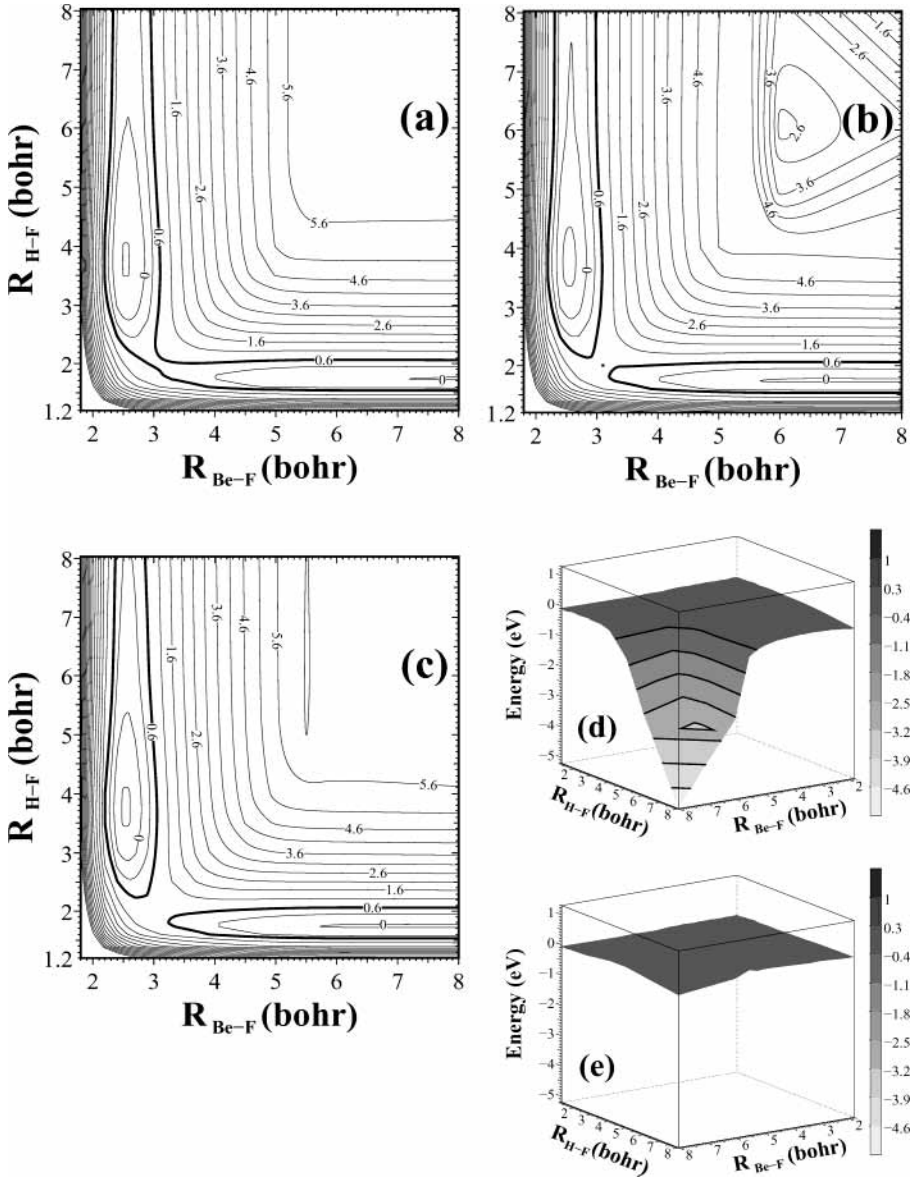

Figure 5. Contour plots for the ground-state PES of the BeFH system, as described by the cc-pVTZ basis set, at $\theta = 70°$, calculated with the MRCI(Q) (a), CCSD(T) (b), and CR-CCSD(T) (c) methods and the dependence of the differences between the CCSD(T) and MRCI(Q) (d) and CR-CCSD(T) and MRCI(Q) (e) energies for $\theta = 70°$ on the Be−F and H−F internuclear separations, R_{Be-F} and R_{H-F}, respectively. All energies are reported in electronvolts relative to the Be + HF reactants ($R_{Be-F} = 50.0$ bohr and $R_{H-F} = 1.7325$ bohr). The thick contour line at 0.6 eV, shown in (a−c), separates the region where the contour spacing is 0.3 eV from the region where the contour spacing is 0.5 eV. The error energy scales on the right side of (d) and (e) are in electronvolts.

energies on θ (see Tables 1 and 2). The CCSD(T) approach behaves in a completely different manner. For CCSD(T), the maximum absolute errors, relative to MRCI(Q), dramatically increase as θ decreases, reaching the huge value of 10.988 eV when $R_{Be-F} = 8.0$ bohr, $R_{H-F} = 8.0$ bohr, and $\theta = 45°$ (see Table 2 and Figure 6d). It can be seen from Figures 1−6 and Tables 1 and 2 that for the CCSD(T) method the errors in the region of larger Be−F and H−F bond distances monotonically increase as the Be−F−H angle decreases. Another difference between the behavior of the CCSD and CCSD(T) methods for $\theta = 45°-180°$ is the fact that the CCSD PES is located above the MRCI(Q) PES, whereas the CCSD(T) PES is usually below the MRCI(Q) PES (see, for example, Figures 1d, 2d, 3d, 4d, 5d, and 6d). One should also notice that for significantly bent geometries ($\theta \leq 90°$), stretching the Be−F bond has a larger effect on the results of the standard CCSD(T) calculations than stretching the H−F bond. This behavior is best illustrated by the results for $\theta = 70°$, which show that when the Be−F bond is stretched to 3.1−5.0 bohr and all H−F distances are considered, the maximum absolute error in the CCSD(T) results is 0.294 eV, whereas when the H−F bond is stretched to 3.0−5.0 bohr and all Be−F distances are considered, the maximum unsigned error in the CCSD(T) energies is 2.581 eV (see Table 2). The above failures of the CCSD and CCSD(T) methods to produce high quality PESs for the BeFH system and the highly nonuniform distribution of errors when the Be−F and H−F distances and the Be−F−H angle vary, observed in the CCSD(T) calculations, are in sharp contrast with the results of the CR-CCSD(T) calculations for which the errors relative to MRCI(Q) remain small for all bond distances and angles. It is remarkable to observe a small increase in the maximum unsigned error characterizing the CR-CCSD(T) calculations with the decreasing values of θ, from 0.180 eV for $\theta = 180°$ to 0.407 eV for $\theta = 45°$ (see Tables 1 and 2). If we limited ourselves to the Be−F−H angles from the $\theta = 70°-180°$ region, the maximum absolute errors in the CR-CCSD(T) results would

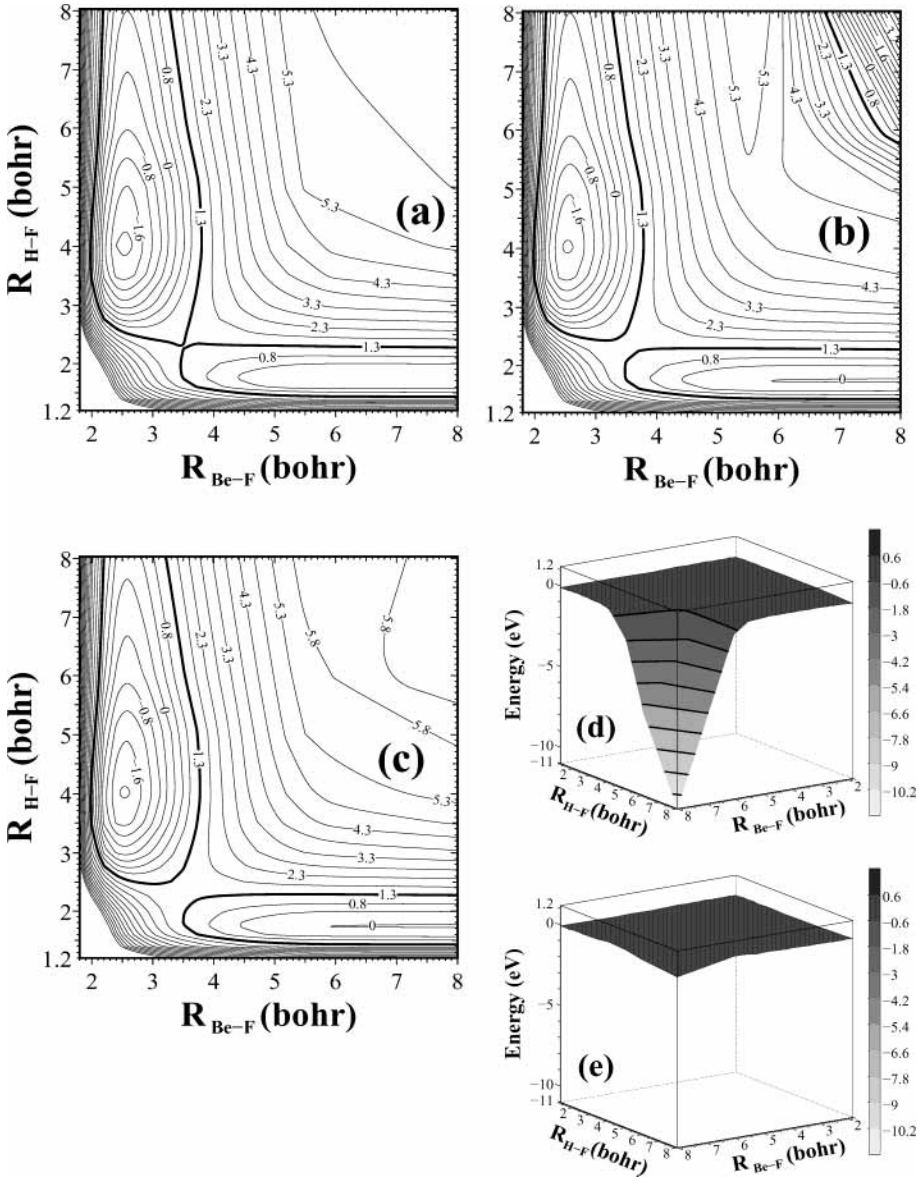

Figure 6. Contour plots for the ground-state PES of the BeFH system, as described by the cc-pVTZ basis set, at $\theta = 45°$, calculated with the MRCI(Q) (a), CCSD(T) (b), and CR-CCSD(T) (c) methods and the dependence of the differences between the CCSD(T) and MRCI(Q) (d) and CR-CCSD(T) and MRCI(Q) (e) energies for $\theta = 45°$ on the Be−F and H−F internuclear separations, R_{Be-F} and R_{H-F}, respectively. All energies are reported in electronvolts relative to the Be + HF reactants ($R_{Be-F} = 50.0$ bohr and $R_{H-F} = 1.7325$ bohr). The thick contour line at 1.3 eV, shown in a−c, separates the region where the contour spacing is 0.4 eV from the region where the contour spacing is 0.5 eV. The error energy scales on the right side of (d) and (e) are in electronvolts.

be very small and virtually independent of θ (they would fluctuate around 0.2 eV). Another useful characteristic of the CR-CCSD(T) approach is its quasi-variational character. As in the case of $\theta = 180°$, the CR-CCSD(T) PES is located slightly above the MRCI(Q) PES when R_{Be-F} and R_{H-F} vary from 1.8 and 1.2 bohr, respectively, to 8.0 bohr and when θ ranges between 45° and 180° (see, for example, Figures 1e, 2e, 3e, 4e, 5e, and 6e).

Essentially all of the remarks that we have made about the relative performance of the CCSD, CCSD(T), CR-CCSD(T), and MRCI(Q) methods for $\theta = 180°$ apply to other values of θ. The CR-CCSD(T) approach eliminates the unphysical features (humps, artificial minima and maxima, etc.) on the CCSD(T) PES for all values of θ (see Figures 2−6). The PES of the BeFH system for $\theta = 90°$ is a good illustration of how the CR-CCSD(T) approach can give results that mirror those of the MRCI(Q) method, even though the standard CCSD(T) approach gives results that are qualitatively incorrect (see Figure 3 and Table 2). The CCSD(T) method not only shows large errors at stretched Be−F and H−F bond distances (up to 4.142 eV; cf. Table 2 and Figure 3d), but it also produces an artificial, ∼2.5 eV deep, well near $R_{Be-F} = 6.0$ bohr and $R_{H-F} = 6.0$ bohr, which can be clearly seen by examining the thin contour line at 3 eV in this region of the CCSD(T) PES in Figure 3b. This well does not appear on either the MRCI(Q) or CR-CCSD(T) PESs. Furthermore, the PESs resulting from the MRCI(Q) and CR-CCSD(T) calculations for $\theta = 90°$ show the formation of a well in the product valley, as is clearly shown by the thin contour lines at 0.09 and 0.23 eV in Figure 3a,c, respectively. This well is due to the beryllium atom beginning to insert between the hydrogen and fluorine atoms, and it does not appear on the CCSD(T) PES at $\theta = 90°$. At $\theta = 90°$, the CCSD(T) PES shows a continuous decrease in energy in the BeF + H product valley as the H−F distance increases, as can be seen in Figure 3b, until the energy of the BeF + H products drops below that of the reactants. Only when the angle θ drops

TABLE 2: Maximum Absolute Errors (in Electronvolts), Relative to MRCI(Q), in the CCSD, CCSD(T), and CR-CCSD(T) Energies for the Ground-State PES of the BeFH System at Be−F−H Angles θ of 135°, 90°, 80°, 70°, and 45°, Calculated with the cc-pVTZ Basis Set[a]

			maximum absolute error					
θ	method	all geometries	$R_{Be-F} \leq 3.1$	$3.1 < R_{Be-F} \leq 5.0$	$5.0 < R_{Be-F}$	$R_{H-F} \leq 3.0$	$3.0 < R_{H-F} \leq 5.0$	$5.0 < R_{H-F}$
135°	CCSD	1.152	0.599	0.804	1.152	0.636	0.868	1.152
	CCSD(T)	3.435	0.401	0.641	3.435	0.260	0.913	3.435
	CR-CCSD(T)	0.184	0.160	0.184	0.150	0.150	0.164	0.184
90°	CCSD	1.199	0.510	0.835	1.199	0.587	0.984	1.199
	CCSD(T)	4.142	0.312	0.599	4.142	0.111	1.653	4.142
	CR-CCSD(T)	0.222	0.160	0.222	0.212	0.144	0.222	0.212
80°	CCSD	1.218	0.469	0.776	1.218	0.554	1.026	1.218
	CCSD(T)	4.519	0.279	0.404	4.519	0.100	2.083	4.519
	CR-CCSD(T)	0.239	0.159	0.214	0.239	0.131	0.214	0.239
70°	CCSD	1.284	0.436	0.707	1.284	0.530	0.987	1.284
	CCSD(T)	5.168	0.236	0.294	5.168	0.098	2.581	5.168
	CR-CCSD(T)	0.286	0.156	0.216	0.286	0.117	0.214	0.286
45°	CCSD	1.184	0.404	0.569	1.184	0.526	1.034	1.184
	CCSD(T)	10.988	0.115	0.108	10.988	0.097	1.676	10.988
	CR-CCSD(T)	0.407	0.132	0.178	0.407	0.110	0.107	0.407

[a] The R_{Be-F} and R_{H-F} values are in bohr.

below 90° do we begin to observe the proper formation of the deep minimum corresponding to the insertion of the Be atom into the H−F bond that leads to the appearance of the HBeF molecule in the $R_{H-F} \approx 4.0-5.0$ bohr and $R_{Be-F} \approx 2.5$ bohr region of the CCSD(T) PES (see Figures 4b, 5b, and 6b). But then, the region of larger H−F and Be−F distances is no longer correctly described by the CCSD(T) approach, as shown, for example, in Figure 6b for $\theta = 45°$. At $\theta = 45°$, the CCSD(T) energies in the $R_{H-F} \geq 5.0$ bohr and $R_{Be-F} \geq 6.0$ bohr region rapidly decrease below the energy of the Be + HF reactants as the H−F and Be−F distances increase (cf. the vicinity of the thick contour line at 1.3 eV in the top right corner of Figure 6b). This behavior is not seen in the MRCI(Q) and CR-CCSD(T) calculations. In analogy to other θ angles, the MRCI(Q) and CR-CCSD(T) energies for $\theta = 45°$ increase with the simultaneous increase of R_{H-F} and R_{Be-F} and the MRCI(Q) and CR-CCSD(T) PESs stabilize at ∼5.8 eV above the Be + HF reactants in the region of large H−F and Be−F distances corresponding to the noninteracting Be + F + H atom limit (see Figure 6a,c). Thus, the CR-CCSD(T) and MRCI(Q) approaches are capable of correctly describing the formation of the deep minimum in the $R_{H-F} \approx 5.0$ bohr and $R_{Be-F} \approx 2.5$ bohr region that corresponds to the HBeF product molecule, as θ approaches 0° and Be inserts itself into the H−F bond, while providing a correct description of other regions of the PES of BeFH. The CCSD(T) approach can capture only some elements of the above insertion process, while producing a completely erratic description of the BeFH PES topology in other regions.

The Results of the CCSD, CCSD(T), CR-CCSD(T), and MRCI(Q) Calculations with the cc-pVTZ Basis Set for $\theta = 0°$. The Be−F−H angle of 0° includes both the beryllium atom inserted between the hydrogen and fluorine atoms (Figure 7 and Table 3) and the beryllium atom approaching the hydrogen atom of the HF molecule to form BeH + F (Figure 8 and Table 4). Let us first discuss the case of the insertion of Be into the H−F bond.

Once again, the PES calculated with the standard CCSD(T) approach is qualitatively incorrect when the Be−F and Be−H distances are stretched, as can be seen from Table 3 and Figure 7d. The unsigned errors for the CCSD(T) method, relative to MRCI(Q), grow to 1.321 eV, when $R_{Be-F} = 6.0$ bohr and $R_{Be-H} = 8.0$ bohr. This should be contrasted with the behavior of the CR-CCSD(T) approach, for which the errors relative to MRCI(Q) do not exceed 0.4 eV when all geometries are examined (cf. Table 3 and Figure 7e). For the majority of the Be−F and Be−H distances included in our calculations for the $\theta = 0°$ case corresponding to the insertion of Be into the H−F bond, the differences between the CR-CCSD(T) and MRCI(Q) energies do not exceed 0.1−0.2 eV (cf. Table 3) and they are often on the order of 0.01−0.1 eV.

In the region of the deep insertion minimum, corresponding to the formation of the HBeF linear molecule, the PESs calculated with the MRCI(Q), CCSD(T), and CR-CCSD(T) methods are all very similar (see Figure 7a−c). The MRCI(Q) energy at the HBeF minimum ($R_{Be-F} = 2.59$ bohr and $R_{Be-H} = 2.49$ bohr), relative to the Be + HF reactants, is −3.98 eV. The CR-CCSD(T) and CCSD(T) energies at the corresponding HBeF minima ($R_{Be-F} = 2.58$ bohr and $R_{Be-H} = 2.49$ bohr for CR-CCSD(T) and $R_{Be-F} = 2.59$ bohr and $R_{Be-H} = 2.49$ bohr for CCSD(T)) are −3.93 and −3.92 eV, respectively. Although the CCSD(T) energy at the HBeF minimum differs from that of MRCI(Q) by only 0.06 eV, the overall topology of the CCSD(T) PES shown in Figure 7b is incorrect. The CCSD(T) PES lies above the MRCI(Q) PES near the HBeF minimum and drops below the MRCI(Q) PES as the Be−H bond is stretched (see, for example, Figure 7d). This is not the case for the CR-CCSD(T) PES, which lies above and is nearly parallel to the MRCI(Q) PES (cf. Figure 7a,c,e).

The second $\theta = 0°$ case of the Be atom reacting with the HF molecule by approaching it from the hydrogen side is another example, much like the cases of $\theta = 45°-180°$, of how the CR-CCSD(T) method can give correct results where the CCSD(T) approach gives an unphysical description (see Figure 8 and Table 4). The CCSD(T) PES shows an artificially low and artificially well pronounced barrier for the formation of the BeH + F products of ∼3 eV in the region of $R_{Be-H} = 2.5$ bohr and $R_{H-F} = 3.5$ bohr (see Figure 8b). At $\theta = 0°$, this barrier is much higher in energy and almost completely flat in the MRCI(Q) and CR-CCSD(T) cases (cf. Figure 8a,c).

As shown in Table 4 and Figure 8d, the unsigned errors in the CCSD(T) results, relative to MRCI(Q), become considerably larger as the H−F bond distance is increased and the Be−H bond distance is decreased. These errors increase to 2.773 eV, obtained for $R_{Be-H} = 1.8$ bohr and $R_{H-F} = 4.0$ bohr. As in other cases, the CCSD approach displays a smaller variation of errors, although again the largest error in the CCSD results relative to MRCI(Q) of 0.980 eV is observed in the region of

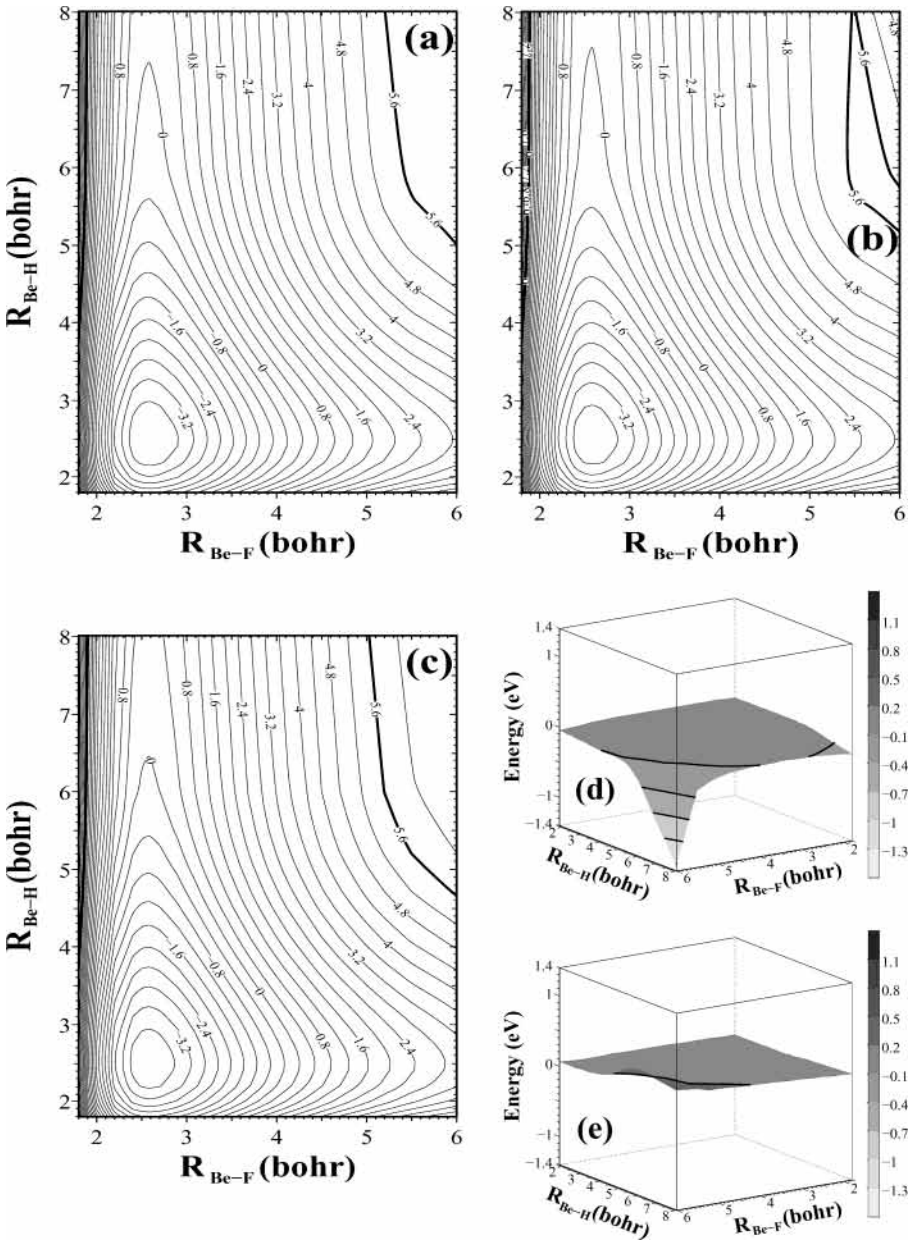

Figure 7. Contour plots for the ground-state PES of the BeFH system, as described by the cc-pVTZ basis set, for the $\theta = 0°$ case corresponding to the Be atom located between H and F, calculated with the MRCI(Q) (a), CCSD(T) (b), and CR-CCSD(T) (c) methods and the dependence of the differences between the CCSD(T) and MRCI(Q) (d) and CR-CCSD(T) and MRCI(Q) (e) energies for the $\theta = 0°$ case, where Be is between H and F, on the Be−F and Be−H internuclear separations, R_{Be-F} and R_{Be-H}, respectively. All energies are reported in electronvolts relative to the Be + HF reactants ($R_{Be-F} = 50.0$ bohr and $R_{H-F} = 1.7325$ bohr). A contour spacing of 0.4 eV is used throughout the plots. The error energy scales on the right side of (d) and (e) are in electronvolts.

TABLE 3: Maximum Absolute Errors (in Electronvolts), Relative to MRCI(Q), in the CCSD, CCSD(T), and CR-CCSD(T) Energies for the Ground-State PES of the BeFH System at a Be−F−H Angle θ of 0° (Be Inserted between F and H), Calculated with the cc-pVTZ Basis Set[a]

		maximum absolute error					
method	all geometries	$R_{Be-F} \leq 3.1$	$3.1 < R_{Be-F} \leq 5.0$	$5.0 < R_{Be-F}$	$R_{Be-H} \leq 3.0$	$3.0 < R_{Be-H} \leq 5.0$	$5.0 < R_{Be-H}$
CCSD	1.303	0.379	0.640	1.303	0.493	0.847	1.303
CCSD(T)	1.321	0.166	0.167	1.321	0.065	0.112	1.321
CR-CCSD(T)	0.398	0.154	0.225	0.398	0.080	0.259	0.398

[a] The R_{Be-F} and R_{Be-H} values are in bohr.

shorter Be−H and H−F distances. The large errors in the CCSD and CCSD(T) results are considerably reduced by the CR-CCSD(T) approach (see Table 4 and Figure 8e). For example, the 2.773 eV maximum error characterizing the standard CCSD(T) calculation for the collinear Be + HF → BeH + F reaction reduces to 0.428 eV, when the CR-CCSD(T) method is employed (cf. Table 4) and for most geometries shown in Figure 8, the differences between the CR-CCSD(T) and MRCI(Q) energies are on the order of 0.01−0.1 eV.

Saddle Points Obtained with the cc-pVTZ Basis Set. The energies and geometries of the saddle points corresponding to several angles θ between 45° and 180°, resulting from the

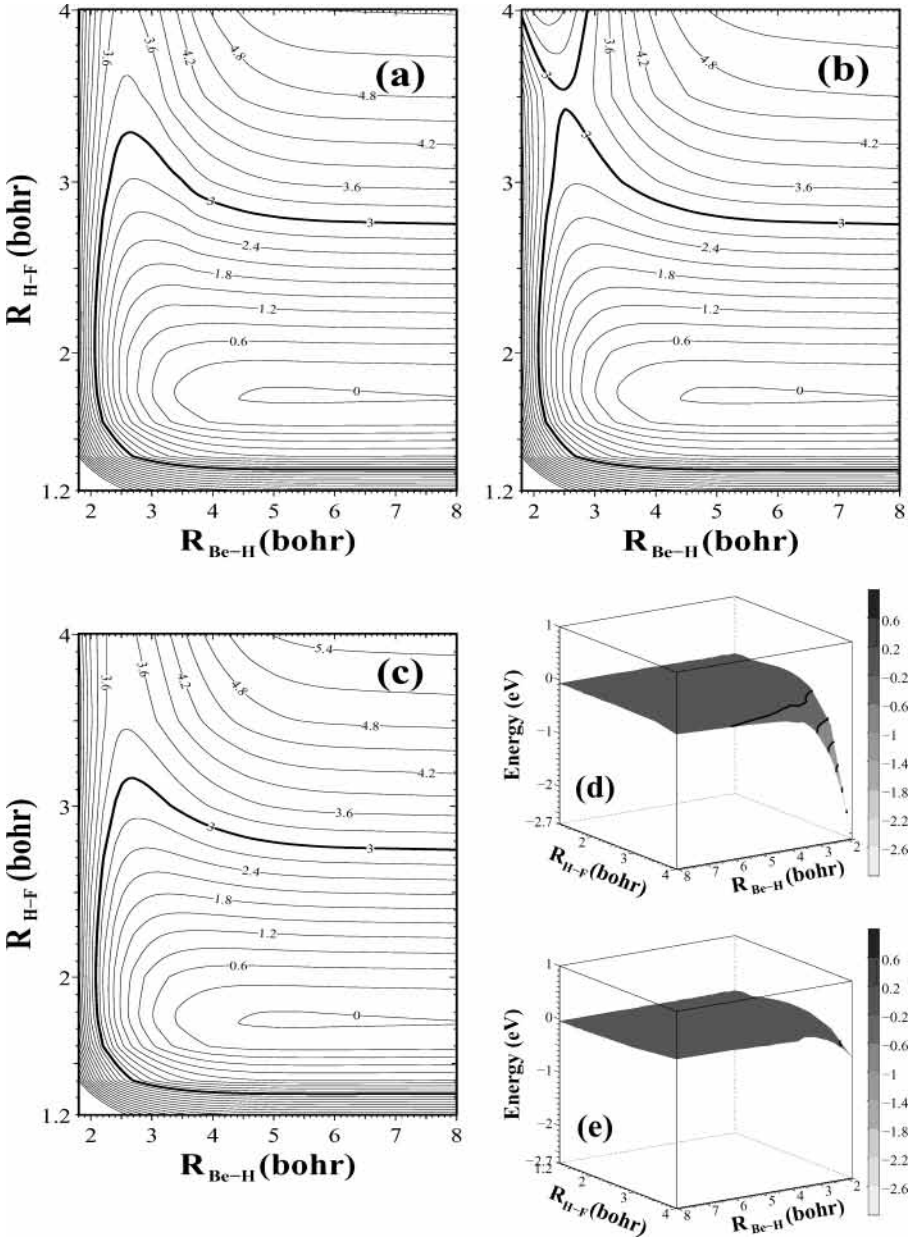

Figure 8. Contour plots for the ground-state PES of the BeFH system, as described by the cc-pVTZ basis set, for the $\theta = 0°$ case corresponding to the H atom located between Be and F, calculated with the MRCI(Q) (a), CCSD(T) (b), and CR-CCSD(T) (c) methods and the dependence of the differences between the CCSD(T) and MRCI(Q) (d) and CR-CCSD(T) and MRCI(Q) (e) energies for the $\theta = 0°$ case, where H is between Be and F, on the Be−H and H−F internuclear separations, R_{Be-H} and R_{H-F}, respectively. All energies are reported in electronvolts relative to the Be + HF reactants ($R_{Be-F} = 50.0$ bohr and $R_{H-F} = 1.7325$ bohr). A contour spacing of 0.3 eV is used throughout the plots. The thick contour line at 3 eV accentuates the presence of an artificially low and artificially well pronounced barrier on the CCSD(T) PES in the region where none is present. The error energy scales on the right side of (d) and (e) are in electronvolts.

TABLE 4: Maximum Absolute Errors (in Electronvolts), Relative to MRCI(Q), in the CCSD, CCSD(T), and CR-CCSD(T) Energies for the Ground-State PES of the BeFH System at a Be−F−H Angle θ of 0° (Be Approaching the H Atom of the HF Molecule), Calculated with the cc-pVTZ Basis Set[a]

		maximum absolute error					
method	all geometries	$R_{Be-H} \leq 3.1$	$3.1 < R_{Be-H} \leq 5.0$	$5.0 < R_{Be-H}$	$R_{H-F} \leq 2.0$	$2.0 < R_{H-F} \leq 3.0$	$3.0 < R_{H-F}$
CCSD	0.980	0.980	0.815	0.592	0.421	0.695	0.980
CCSD(T)	2.773	2.773	0.545	0.228	0.070	0.140	2.773
CR-CCSD(T)	0.428	0.428	0.136	0.109	0.069	0.131	0.428

[a] The R_{Be-H} and R_{H-F} values are in bohr.

CCSD(T), CR-CCSD(T), and MRCI(Q) calculations employing the cc-pVTZ basis set, are shown in Table 5 (cf. also, Figure 9). As can be seen in Table 5 and Figure 9, at larger values of θ, the energies of the saddle points calculated with the CCSD(T) method are below those obtained with the MRCI(Q) approach, while at smaller θ values this trend is reversed, i.e., the CCSD(T) energy barriers are greater than their MRCI(Q) counterparts. For example, at $\theta = 180°$ the CCSD(T) approach produces an energy barrier of 1.30 eV, while the MRCI(Q) approach gives a barrier height of 1.35 eV. For $\theta = 135°$, the CCSD(T) barrier

TABLE 5: Energies (E) and Geometries (R_{Be-F} and R_{H-F}) of the Saddle Points on the BeFH PES for the Be−F−H Angles θ = 45°, 70°, 80°, 90°, 135°, and 180°, and Energies (E) and Geometries (R_{Be-F} and R_{Be-H}) of the HBeF Insertion Minimum Resulting from the CCSD(T), CR-CCSD(T), and MRCI(Q) Calculations with the cc-pVTZ Basis Set[a]

θ	quantity	CCSD(T)	CR-CCSD(T)	MRCI(Q)
45°	E	1.36	1.41	1.30
	R_{Be-F}	3.51	3.50	3.52
	R_{H-F}	2.35	2.35	2.34
70°	E	0.61	0.64	0.58
	R_{Be-F}	2.98	2.96	3.01
	R_{H-F}	2.05	2.06	2.03
80°	E	0.60	0.65	0.57
	R_{Be-F}	2.78	2.77	2.79
	R_{H-F}	2.20	2.22	2.18
90°	E	0.83	0.79	0.71
	R_{Be-F}	2.72	2.71	2.72
	R_{H-F}	2.31	2.34	2.30
135°	E	1.19	1.29	1.22
	R_{Be-F}	2.76	2.74	2.76
	R_{H-F}	2.31	2.36	2.30
180°	E	1.30	1.40	1.35
	R_{Be-F}	2.80	2.79	2.81
	R_{H-F}	2.29	2.34	2.28
0° (HBeF minimum)	E	−3.92	−3.93	−3.98
	R_{Be-F}	2.59	2.58	2.59
	R_{Be-H}	2.49	2.49	2.49

[a] Energies are in electronvolts, Relative to the Be + HF asymptote, and internuclear separations are in bohr.

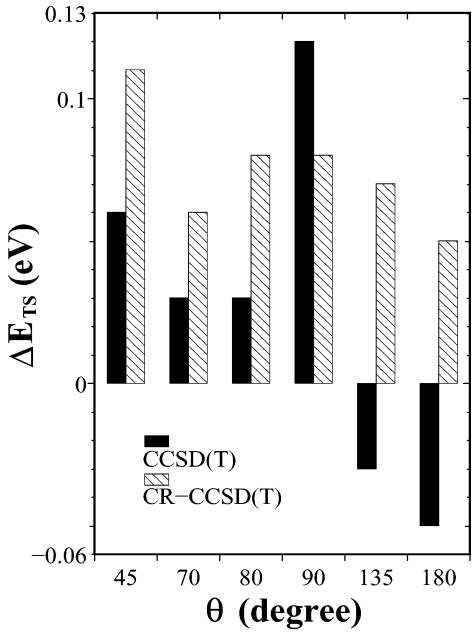

Figure 9. Dependence of the differences between the CCSD(T) and MRCI(Q) saddle point energies (solid bars) and CR-CCSD(T) and MRCI(Q) saddle point energies (half-filled bars) for the BeFH system, as described by the cc-pVTZ basis set, on the Be−F−H angle θ.

is 0.03 eV below the MRCI(Q) result. In the θ = 45°−90° region, the CCSD(T) values of the saddle point energies are 0.03−0.12 eV above the corresponding MRCI(Q) values. In fact, the CCSD(T) saddle point energy at θ = 90° is above the corresponding MRCI(Q) and CR-CCSD(T) values. An entirely different pattern is observed in the CR-CCSD(T) calculations. The CR-CCSD(T) method produces saddle point energies that are invariably above the corresponding MRCI(Q) values for all θ values. The differences between the CR-CCSD(T) and MRCI(Q) saddle point energies are always positive and range between 0.05 and 0.11 eV.

The above patterns confirm our earlier observation that the CR-CCSD(T) and MRCI(Q) PESs are virtually parallel and very close to each other. This is reflected by the small positive and almost constant differences between the saddle point energies obtained in the CR-CCSD(T) and MRCI(Q) calculations at all θ values. The fact that the CCSD(T) saddle point energies fluctuate around the MRCI(Q) values, being below the MRCI(Q) values at larger angles θ and above the MRCI(Q) saddle point energies at smaller angles θ, shows once again that the CCSD(T) and MRCI(Q) PESs are not parallel. Although both CCSD(T) and CR-CCSD(T) methods give small unsigned errors in the calculated saddle point energies, it is better to use an approach that is capable of producing small errors and PESs that are parallel to the virtually exact PES, obtained in this case with the MRCI(Q) approach. The CR-CCSD(T) method is in this category.

The PES for the Collinear Be + HF → BeF + H Reaction (θ = 180°) Obtained with the cc-pVQZ Basis Set. The PESs for the collinear, θ = 180°, BeFH system calculated with the CCSD(T), CR-CCSD(T), and MRCI(Q) approaches and the cc-pVQZ basis set are shown in Figure 10. It is clear from Figure 10 that, as in the cc-pVTZ case (cf. Figure 1), the PES calculated with the CCSD(T) approach is completely pathological when compared to the PES calculated with the MRCI(Q) method. At large Be−F and H−F separations, the errors in the CCSD(T) energies, relative to MRCI(Q), increase to 4.077 eV (see Table 1) and the CCSD(T) PES goes significantly below the MRCI(Q) PES (see Figure 10d). This should be contrasted with the small, 0.198 eV, maximum error obtained with the CR-CCSD(T) approach and the virtually perfect agreement between the MRCI(Q) and CR-CCSD(T) PESs shown in Figure 10a,c, respectively (cf. also, Figure 10e). The PES calculated with the CR-CCSD(T) method is nearly identical to the PES calculated with the MRCI(Q) method, and the CR-CCSD(T) approach eliminates the catastrophic failure and nonvariational behavior of the CCSD(T) approach in the region of stretched Be−F and H−F (particularly, H−F) distances (cf. Figure 10d,e). As in the cc-pVTZ case, the CCSD(T) method produces a saddle point that is too low in energy, when compared to the MRCI(Q) and CR-CCSD(T) results. The BeF + H product valley resulting from the CR-CCSD(T)/cc-pVQZ calculations is slightly above and almost parallel to the product valley on the analogous MRCI(Q) PES, while the product valley on the CCSD(T) PES is too low in energy, with energies in the region of larger H−F distances dropping significantly below the energy of the Be + HF reactants. The CR-CCSD(T) and MRCI(Q) product valleys are shaped in almost identical ways, whereas there is a significant difference between the CCSD(T) and MRCI(Q) PESs in the region behind the barrier where the BeF + H products are formed. All of this can be seen by examining the thick contour line at 1.3 eV in Figure 10 and by noticing that the thin contour line at 0 eV, which is clearly visible in the CCSD(T) contour plot shown in Figure 10b, does not appear in the product valley of the CR-CCSD(T) and MRCI(Q) PESs. In addition, the endothermicity of the Be + HF → BeF + H reaction obtained with the CCSD(T) approach and the cc-pVQZ basis set of −0.051 eV has the wrong sign when compared to the MRCI(Q) endothermicity of 0.099 eV. The CR-CCSD(T) endothermicity of 0.301 eV has the correct sign and is in reasonable agreement with the experimentally derived value of 0.193 eV, obtained using the dissociation energies of HF and BeF.

A Comparison of the CR-CCSD(T) Results for the Collinear Be + HF → BeF + H Reaction (θ = 180°)

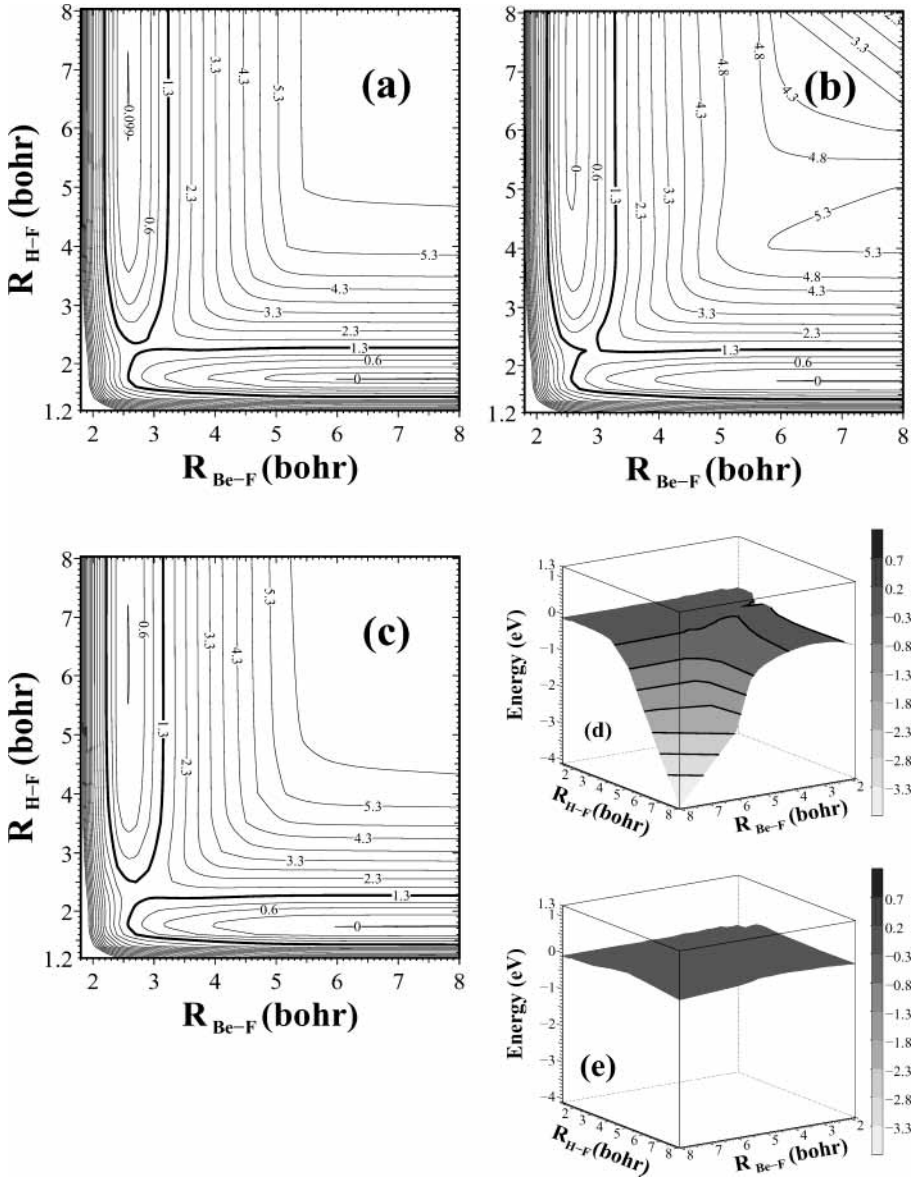

Figure 10. Contour plots for the ground-state PES of the BeFH system, as described by the cc-pVQZ basis set, at $\theta = 180°$, calculated with the MRCI(Q) (a), CCSD(T) (b), and CR-CCSD(T) (c) methods and the dependence of the differences between the CCSD(T) and MRCI(Q) (d) and CR-CCSD(T) and MRCI(Q) (e) energies for $\theta = 180°$ on the Be−F and H−F internuclear separations, R_{Be-F} and R_{H-F}, respectively. All energies are reported in electronvolts relative to the Be + HF reactants ($R_{Be-F} = 8.0$ bohr and $R_{H-F} = 1.7325$ bohr). The thick contour line at 1.3 eV, shown in (a−c), separates the region where the contour spacing is 0.3 eV from the region where the contour spacing is 0.5 eV. An extra contour line corresponding to 0.099 eV has been added to (a) to better describe the product channel. The error energy scales on the right side of (d) and (e) are in electronvolts.

Obtained Using the cc-pVTZ and cc-pVQZ Basis Sets with the Previously Published Results Obtained with the MIDI Basis Set. As mentioned in the Introduction, the CR-CCSD(T) PES for the collinear Be + HF → BeF + H reaction has been obtained earlier using a small, MIDI, basis set.[39] The use of the MIDI basis set allowed the authors of ref 39 to compare the CCSD(T) and CR-CCSD(T) PESs with the exact PES obtained with the full CI method. A comparison of the results reported in ref 39 with those obtained in this work shows that the main conclusions of the small basis set study[39] regarding the relative performance of the CCSD(T) vs CR-CCSD(T) methods do not depend on the basis set. Thus, independent of the basis set employed, the CCSD(T) PES has the wrong topology, particularly in the product valley and in the region where both Be−F and H−F bonds are stretched, which is corrected by the CR-CCSD(T) approach. Independent of the basis set employed, the CR-CCSD(T) PES is slightly above and virtually parallel to the exact, full CI, or virtually exact, MRCI(Q), PESs, whereas the CCSD(T) PES is, for the most part, far from being parallel to the full CI or MRCI(Q) PESs and significantly below the latter two PESs.

As shown in Table 1, the absolute values of errors in the CCSD, CCSD(T), and CR-CCSD(T) results, relative to full CI or MRCI(Q), depend on the basis set, although the differences between the errors obtained with the cc-pVTZ and cc-pVQZ basis sets are already rather small, implying that the results obtained in this work are close to the basis set limit in these two cases, particularly when the CR-CCSD(T) method is examined. Typically, the unsigned errors resulting from the calculations with the MIDI basis set are 2−4 times smaller than the errors resulting from the calculations using the cc-pVTZ and cc-pVQZ basis sets, since the number of unoccupied orbitals dramatically increases as we go from the MIDI basis set to the cc-pVTZ and cc-pVQZ basis sets, but the overall error patterns

observed in the small and larger basis set calculations are similar (see Table 1). Interestingly enough, the errors in the CR-CCSD(T) results in the region of stretched Be−F and H−F bonds do not grow as rapidly with the basis set as in the CCSD(T) case (cf. the $R_{Be-F} > 5.0$ bohr and $R_{H-F} > 5.0$ bohr region in Table 1), which is another manifestation of the fact that the CR-CCSD(T) approach is much more robust than the CCSD(T) method in the PES regions where the CCSD(T) method fails.

In conclusion, a comparison of the results obtained in this article using the cc-pVTZ and cc-pVQZ basis sets with those obtained earlier with the MIDI basis set[39] shows that the success of the CR-CCSD(T) method in small basis set calculations guarantees the successful performance of this method in realistic calculations employing large basis sets.

Summary

The CR-CCSD(T) method has been used to calculate the entire ground-state PES for the Be + HF reaction. The cc-pVTZ and cc-pVQZ basis sets have been employed. The resulting PESs have been compared with the PESs obtained with the CCSD, CCSD(T), and MRCI(Q) methods. In addition to the collinear Be + HF → BeF + H reaction, several angles of approach of the HF molecule by the Be atom, leading to the formation of the BeF + H, BeH + F, and HBeF products, have been examined.

It has been shown that the single-reference "black-box" CR-CCSD(T) method employing the spin- and symmetry-adapted RHF reference provides a highly accurate PES of the BeFH system, which is almost identical to the PES resulting from the more expensive and more complicated MRCI(Q) calculations. The CR-CCSD(T) approach eliminates large errors and pathologies observed in the standard CCSD and CCSD(T) calculations. In particular, the CR-CCSD(T) method eliminates the nonvariational collapse of the CCSD(T) approach in regions of the PES corresponding to larger internuclear separations without making the calculations significantly more expensive or difficult to perform. Unlike the CCSD and CCSD(T) PESs, the CR-CCSD(T) PES is close and virtually parallel to the MRCI(Q) PES and has the correct topology, enabling us to understand the formation of different reaction products that the interaction of the Be atom with HF can lead to.

The relatively low cost and ease-of-use of the CR-CCSD(T) method, when compared to the advanced multireference techniques, such as MRCI(Q), which would usually be used to calculate accurate reactive PESs, along with its high accuracy, make the CR-CCSD(T) method an attractive alternative for studies of chemical reactions proceeding on singlet PESs, where single bonds are broken and formed. Work is in progress toward extending the highly efficient CR-CCSD(T) computer programs[37] in GAMESS to nonsinglet PESs. The preliminary results for bond breaking on doublet PESs, employing the ROHF references, have already been reported,[32] and we hope to extend these studies to exchange chemical reactions proceeding on doublet and triplet PESs soon.

Acknowledgment. This work has been supported by the U.S. Department of Energy, Office of Basic Energy Sciences, SciDAC Computational Chemistry Program (Grant No. DE-FG02-01ER15228), by the Alfred P. Sloan Foundation, and by the National Science Foundation (under Grant No. CHE-0309517).

Supporting Information Available: Tables with the CCSD, R-CCSD(T), CR-CCSD(T), and MRCI(Q) energies for all nuclear geometries of the BeFH system considered in this study. This material is available free of charge via the Internet at http://pubs.acs.org.

References and Notes

(1) (a) Kuntz, P. J.; Roach, A. C. *J. Chem. Phys.* **1981**, *74*, 3420. (b) Roach, A. C.; Kuntz, P. J. *J. Chem. Phys.* **1981**, *74*, 3435. (c) Kuntz, P. J.; Schreiber, J. L. *J. Chem. Phys.* **1982**, *76*, 4120.

(2) Aguado, A.; Sanz, V.; Paniagua, M. *Int. J. Quantum Chem.* **1997**, *61*, 491.

(3) Schor, H.; Chapman, S.; Green, S.; Zare, R. N. *J. Chem. Phys.* **1978**, *69*, 3790.

(4) Chapman, S.; Dupuis, M.; Green, S. *Chem. Phys.* **1983**, *78*, 93.

(5) Garcia, E.; Lagana, A. *Mol. Phys.* **1985**, *56*, 629.

(6) Liu, X.; Murrell, J. N. *J. Chem. Soc., Faraday Trans.* **1991**, *87*, 435.

(7) Aguado, A.; Sieiro, C.; Paniagua, M. *J. Mol. Struct. (THEOCHEM)* **1992**, *260*, 179.

(8) Keller, A.; Visticot, J. P.; Tsuchiya, S.; Zwier, T. S.; Duval, M. C.; Jouvet, C.; Soep, B.; Whitham, C. J. In *Dynamics of Polyatomic van der Waals Complexes*; Halberstadt, N., Janda, K. C., Eds.; Plenum: New York, 1990; pp 103−121.

(9) Keller, A.; Lawruszczuk, R.; Soep, B.; Visticot, J. P. *J. Chem. Phys.* **1996**, *105*, 4556.

(10) Skowronek, S.; Gonzalez-Ureña, A. *Prog. React. Kinet. Mech.* **1999**, *24*, 101.

(11) Soep, B.; Whitham, C. J.; Keller, A.; Visticot, J. P. *Faraday Discuss. Chem. Soc.* **1991**, *91*, 191.

(12) Soep, B.; Abbés, S.; Keller, A.; Visticot, J. P. *J. Chem. Phys.* **1991**, *96*, 440.

(13) Lawruszczuk, R.; Elhanine, M.; Soep, B. *J. Chem. Phys.* **1998**, *108*, 8374.

(14) Skowronek, S.; Pereira, R.; Gonzalez-Ureña, A. *J. Chem. Phys.* **1997**, *107*, 1668.

(15) Skowronek, S.; Pereira, R.; Gonzalez-Ureña, A. *J. Phys. Chem. A* **1997**, *101*, 7468.

(16) Stert, V.; Farmanara, P.; Radloff, W.; Noack, F.; Skowronek, S.; Jimenez, J.; Gonzalez-Ureña, A. *Phys. Rev. A* **1999**, *59*, R1727.

(17) Skowronek, S.; Jimenez, J. B.; A. Gonzalez-Ureña, A. *Chem. Phys. Lett.* **1999**, *303*, 275.

(18) Farmanara, P.; Stert, V.; Radloff, W.; Skowronek, S.; Gonzalez-Ureña, A. *Chem. Phys. Lett.* **1999**, *304*, 127.

(19) Skowronek, S.; Jimenez, J. B.; Gonzalez-Ureña, A. *J. Chem. Phys.* **1999**, *111*, 460.

(20) Coester, F. *Nucl. Phys.* **1958**, *7*, 421.

(21) Coester, F.; Kümmel, H. *Nucl. Phys.* **1960**, *17*, 477.

(22) Čížek, J. *J. Chem. Phys.* **1966**, *45*, 4256.

(23) Čížek, J. *Adv. Chem. Phys.* **1969**, *14*, 35.

(24) Čížek, J.; Paldus, J. *Int. J. Quantum Chem.* **1971**, *5*, 359.

(25) Piecuch, P.; Kowalski, K. In *Computational Chemistry: Reviews of Current Trends*; Leszczyński, J., Ed.; World Scientific: Singapore, 2000; Vol. 5, pp 1−104.

(26) (a) Kowalski, K.; Piecuch, P. *J. Chem. Phys.* **2000**, *113*, 18. (b) Kowalski, K.; Piecuch, P. *J. Chem. Phys.* **2000**, *113*, 5644.

(27) Kowalski, K.; Piecuch, P. *J. Mol. Struct. (THEOCHEM)* **2001**, *547*, 191.

(28) Piecuch, P.; Kowalski, K.; Pimienta, I. S. O.; Kucharski, S. A. In *Low-Lying Potential Energy Surfaces*; Hoffman M. R., Dyall, K. G., Eds.; ACS Symposium Series 828; American Chemical Society: Washington, DC, 2002; pp 31−64.

(29) (a) Kowalski, K.; Piecuch, P. *J. Chem. Phys.* **2001**, *115*, 2966. (b) Kowalski, K.; Piecuch, P. *J. Chem. Phys.* **2002**, *116*, 7411.

(30) Piecuch, P.; Kowalski, K.; Pimienta, I. S. O.; McGuire, M. J. *Int. Rev. Phys. Chem.* **2002**, *21*, 527.

(31) Piecuch, P.; Kowalski, K.; Fan, P.-D.; Pimienta, I. S. O. In *Advanced Topics in Theoretical Chemical Physics*; Maruani, J., Lefebvre, R., Brändas, E., Eds.; Progress in Theoretical Chemistry and Physics; Kluwer: Dordrecht, The Netherlands, 2003; Vol. 12, pp 119−206.

(32) Piecuch, P.; Kowalski, K.; Pimienta, I. S. O.; Fan, P.-D.; Lodriguito, M.; McGuire, M. J.; Kucharski, S. A.; Kuś, T.; Musiał, M. *Theor. Chem. Acc.*, in press.

(33) Kowalski, K.; Piecuch, P. *Chem. Phys. Lett.* **2001**, *344*, 165.

(34) Purvis, G. D., III; Bartlett, R. J. *J. Chem. Phys.* **1982**, *76*, 1910.

(35) Raghavachari, K.; Trucks, G. W.; Pople, J. A.; Head-Gordon, M. *Chem. Phys. Lett.* **1989**, *157*, 479.

(36) Piecuch, P.; Kucharski, S. A.; Špirko, V.; Kowalski, K. *J. Chem. Phys.* **2001**, *115*, 176.

(37) Piecuch, P.; Kucharski, S. A.; Kowalski, K.; Musiał, M. *Comput. Phys. Commun.* **2002**, *149*, 71.

(38) Özkan, I.; Kinal, A.; Balci, M. *J. Phys. Chem. A* **2004**, *108*, 507.
(39) McGuire, M. J.; Kowalski, K.; Piecuch, P. *J. Chem. Phys.* **2002**, *117*, 3617.
(40) Huzinaga, S.; Andzelm, J.; Klobukowski, M.; Radzio-Andzelm, E.; Sakai, Y.; Tatewaki, H. *Gaussian Basis Sets for Molecular Calculations*; Elsevier: Amsterdam, 1984.
(41) Dunning, T. H., Jr. *J. Chem. Phys.* **1989**, *90*, 1007.
(42) Schmidt, M. W.; Baldridge, K. K.; Boatz, J. A.; Elbert, S. T.; Gordon, M. S.; Jensen, J. H.; Koseki, S.; Matsunaga, N.; Nguyen, K. A.; Su, S.; Windus, T. L.; Dupuis, M.; Montgomery, J. A. *J. Comput. Chem.* **1993**, *14*, 1347.
(43) Werner, H.-J.; Knowles, P. J. *J. Chem. Phys.* **1988**, *89*, 5803.
(44) Knowles, P. J.; Werner, H.-J. *Chem. Phys. Lett.* **1988**, *145*, 514.
(45) Amos, R. D.; Bernhardsson, A.; Berning, A.; Celani, P.; Cooper, D. L.; Deegan, M. J. O.; Dobbyn, A. J.; Eckert, F.; Hampel, C.; Hetzer, G.; Knowles, P. J.; Korona, T.; Lindh, R.; Lloyd, A. W.; McNicholas, S. J.; Manby, F. R.; Meyer, W.; Mura, M. E.; Nicklass, A.; Palmieri, P.; Pitzer, R.; Rauhut, G.; Schütz, M.; Schumann, U.; Stoll, H.; Stone, A. J.; Tarroni, R.; Thorsteinsson, T.; Werner, H.-J. *MOLPRO*, a package of ab initio programs, version 2002.1.
(46) Huber, K. P.; Herzberg, G. *Molecular Spectra and Molecular Structure*; Constants of Diatomic Molecules; Van Nostrand: New York, 1979; Vol. 4.
(47) Coxon, J. A.; Hajigeorgiou, P. G. *J. Mol. Spectrosc.* **1990**, *142*, 254.
(48) Hildenbrand, D.; Murad, E. *J. Chem. Phys.* **1966**, *44*, 1524.